

Neutron Diffraction Study of  $\text{RbFeF}_3$ <sup>†</sup>

Franklin F. Y. Wang\*

*Department of Materials Science,  
State University of New York at Stony Brook, Stony Brook, New York 11790*

and

D. E. Cox

*Physics Department, Brookhaven National Laboratory, Upton, New York 11973*

and

M. Kestigian

*Sperry Rand Research Center, Sudbury, Massachusetts 01776*

(Received 4 January 1971)

A neutron diffraction study of both unmagnetized polycrystalline and single-crystal samples of  $\text{RbFeF}_3$  at zero applied field has revealed that magnetic order sets in at a Néel point  $T_N$  of  $(100.5 \pm 0.5)$  °K. Below  $T_N$ , magnetic peaks characteristic of the  $G$  type of antiferromagnetic lattice are observed. The value of the ordered moment extrapolated to 0 °K is  $4.6 \pm 0.2 \mu_B$ , and its variation with temperature is reversible and does not exhibit any abrupt changes in the region between 4.6 °K and  $T_N$ , in sharp contrast to the behavior reported for the weak spontaneous moment. Between 84.5 and 100.1 °K, the magnetization is in accord with a critical-scattering relationship having an exponent  $\beta$  of  $0.329 \pm 0.004$ , in close agreement with published Mössbauer measurements.

## I. INTRODUCTION

The perovskite compound  $\text{RbFeF}_3$  has been shown to undergo several crystallographic transitions,<sup>1</sup> in the course of which it exhibits interesting magnetic<sup>1-3</sup> and optical<sup>4,5</sup> properties. At low temperatures, some of these properties such as the complex Mössbauer spectra<sup>3,6-8</sup> and magnetic anisotropy<sup>9</sup> are not well understood. The following general features, have, however, been established, although there are some differences in exact details.

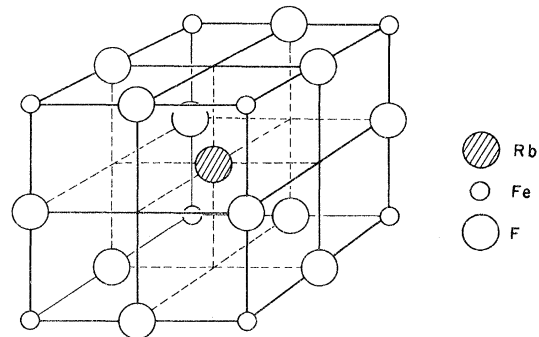
The compound orders antiferromagnetically at about 102 °K, and then undergoes a first-order transition around 86 °K from a tetragonal structure ( $c/a=1.0034$ ) to some lower (probably orthorhombic) symmetry. At this point, a spontaneous moment of about  $0.2 \mu_B$  per Fe ion develops abruptly. There is yet another transition at about 45 °K to a still lower symmetry (probably monoclinic) structure at which there is a further discontinuity in the magnetization. The spontaneous moment extrapolated to 0 °K is of the order of  $0.5 \mu_B$ . Between 45 and 87 °K, the Mössbauer spectra reveal the existence of a hyperfine structure characteristic of two inequivalent sets of Fe sites, in contrast to the regions below 45 °K and between 87 °K and the Néel point, where the spectra are characteristic of a single set of Fe sites. At the Néel point, the symmetry is believed to change from cubic to tetragonal, although in fact a measurable tetragonal distortion ( $c/a=1.0012$ ) was not detected until the temperature reached 97 °K.<sup>1</sup> It is also noteworthy that the low symmetry at 40 °K is not reflected in the optical and magnetic behavior, which is that

expected for cubic symmetry.<sup>9</sup>

In view of this complex behavior, a neutron diffraction study of  $\text{RbFeF}_3$  was undertaken. This paper reports the first part of this study with unpolarized neutrons on both polycrystalline and single crystal samples. Since weakly ferromagnetic properties are frequently dependent on previous magnetic history, these samples were at no time subjected to any external magnetic field other than that of the earth, and are designated "unmagnetized."

## II. EXPERIMENTAL DETAILS AND RESULTS

The polycrystalline  $\text{RbFeF}_3$  samples were prepared by the reaction of  $\text{RbF}$  and  $\text{FeF}_2$  in a He carrier gas containing HF at 1125 °C. Single crystals were grown in graphite vessels by the horizontal Bridgman technique. They were found to be heavily

FIG. 1. Cubic perovskite crystal structure of  $\text{RbFeF}_3$ .

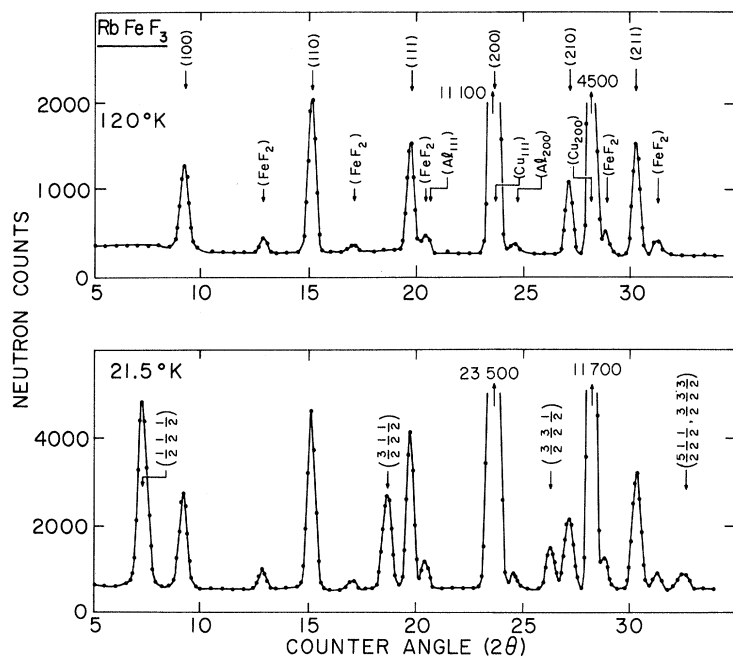


FIG. 2. Neutron diffraction patterns from polycrystalline  $\text{RbFeF}_3$  at 120 and 21.5°K.

twinned, although they appeared transparent under visual observation. However, repeated sectioning and x-ray examination finally yielded a few small single crystals, the largest of which was selected for the neutron diffraction study. It had roughly the shape of a rectangular pillar about  $2 \times 2 \times 4$  mm with the [110] axis approximately parallel to the long dimension. The neutron rocking curve for this crystal had a full width at half-maximum of about 30 min of arc.

X-ray patterns of the polycrystalline material showed a simple cubic pattern characteristic of the perovskite structure, as shown in Fig. 1, with a lattice constant of  $4.174 \pm 0.002 \text{ \AA}$ . In addition, there were a few weak lines of a second phase identified as  $\text{FeF}_2$ . The pattern from a small powdered sample of the single-crystal material showed only a cubic phase with a lattice constant of  $4.179 \pm 0.002 \text{ \AA}$ . Some low-temperature diffractometer traces of this material are currently being exam-

ined in an effort to elucidate the nature of the lower-symmetry phases.<sup>10</sup>

Neutron diffraction experiments were performed at the Brookhaven High Flux Beam Reactor. A neutron beam of wavelength  $1.084 \text{ \AA}$  from the (311) reflection of a germanium monochromator was utilized. Since the (622) reflection is absent,

TABLE I. Parameter values from least-squares refinement of 120°K neutron powder data from  $\text{RbFeF}_3$ . Standard errors are given in parentheses.

$B_{\text{Rb}}$	$0.50 (0.14) \text{ \AA}^2$
$B_{\text{Fe}}$	$0.27 (0.11) \text{ \AA}^2$
$B_{\text{F}}$	$0.66 (0.14) \text{ \AA}^2$
R factor	$\frac{\sum  I_{\text{obs}} - I_{\text{calc}} }{\sum I_{\text{obs}}} = 5.2\%$
Weighted R factor	$\left( \frac{\sum w(I_{\text{obs}} - I_{\text{calc}})^2}{\sum w I_{\text{obs}}^2} \right)^{1/2} = 5.2\%$

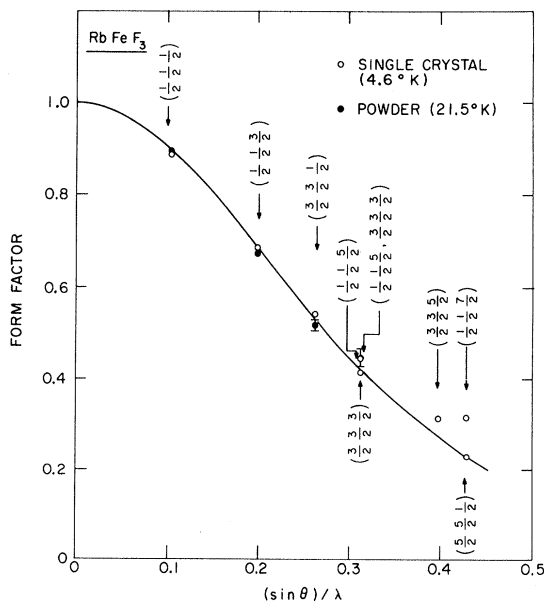


FIG. 3. Magnetic form values for  $\text{Fe}^{2+}$  in  $\text{RbFeF}_3$  determined from single-crystal (4.6°K) and powder neutron diffraction (21.5°K) data. Solid line is the theoretical curve for  $f(j_0)$  (Ref. 15).

TABLE II. Comparison of observed and calculated neutron intensities from polycrystalline RbFeF<sub>3</sub> at 120 °K. Atomic positions as shown in Fig. 1. Scattering amplitudes as listed in text, and temperature factors as listed in Table I.

<i>hkl</i>	<i>I</i> <sub>calc</sub>	<i>I</i> <sub>obs</sub>
100	41.3	45.1
110	76.8	73.8
111	55.5	53.1
200	Overlap with Cu(111)	
210	32.9	34.6
211	51.5	52.5
220	168.2	174.1
221 } 300 }	18.2 } 4.6 }	22.8 } 22.7
310	31.2	29.5
311	40.0	44.6
222	73.1	69.3
320	12.6	11.4
321	45.1	47.7
400	Overlap with Cu(222)	
410 } 322 }	9.6 } 9.6 }	19.2 } 19.0
411 } 330 }	17.8 } 8.9 }	26.7 } 30.3
331	20.5	23.5
420	127.1	131.7
421	Overlap with Cu(400)	
332	14.8	14.0
422	104.7	112.1

second-order wavelength contamination was therefore eliminated, while third-order contamination was found to be negligible. The sample was packed in a  $\frac{3}{8}$ -in. diam copper holder, and was mounted in a Cryogenic Associates variable-temperature Dewar. Temperature was controlled to better than  $\pm 0.1$  °K.

#### A. Polycrystalline Data

A neutron diffraction pattern of the RbFeF<sub>3</sub> powder sample at 120 °K is shown in the top half of Fig. 2. The main peaks in this pattern can all be indexed on the basis of a cubic perovskite cell. The impurity peaks for FeF<sub>2</sub> can also be seen, and

TABLE IV. Comparison of observed and calculated neutron structure factors from single-crystal RbFeF<sub>3</sub> at 120 and 42 °K. Scattering amplitudes as listed in text, and temperature factors as listed in Table IV.

<i>hkl</i>	120 °K		42 °K	
	<i>F</i> <sub>calc</sub>	<i>F</i> <sub>obs</sub>	<i>F</i> <sub>calc</sub>	<i>F</i> <sub>obs</sub>
100	16.7	16.8	16.9	17.1
200	58.4	58.9	63.9	65.7
300	16.0	15.6	16.4	16.0
400	57.0	58.9	63.7	63.5
111	28.3	28.7	29.5	29.6
222	58.1	58.0	64.2	62.7
110	22.5	21.6	22.8	22.3
220	58.9	57.1	64.4	63.9
330	21.2	21.3	22.1	22.2
221	16.0	16.2	16.4	16.9
112	22.3	22.4	22.8	22.7
113	26.4	26.2	29.0	29.0
<i>R</i> factor	1.6%		1.4%	
Weighted	1.4%		1.2%	
<i>R</i> factor				

from a rough intensity calculation, the amount of this impurity was estimated to be about 5%.

A least-squares refinement of the nuclear intensity data was made with a program<sup>11</sup> which permits overlapping reflections to be included. Coherent neutron scattering amplitudes for Rb, Fe, and F were taken as 0.705,<sup>12</sup> 0.951,<sup>13</sup> and 0.56<sup>14</sup> × 10<sup>-12</sup> cm, respectively. The amplitude value for Rb is one which has recently been obtained from a neutron diffraction study of RbCl.<sup>12</sup> Isotropic temperatures *B*<sub>Rb</sub>, *B*<sub>Fe</sub>, and *B*<sub>F</sub> were treated as variable parameters in the refinement, and the final values obtained are listed in Table I. The observed and calculated neutron intensities are in good agreement (Table II). Corrections to the observed intensities have been made where necessary to allow for FeF<sub>2</sub> impurity.

A neutron diffraction pattern of the RbFeF<sub>3</sub> powder sample at 21.5 °K is shown in the lower-half of Fig. 2. The intensities of the nuclear peaks remain essentially unchanged, although the higher-angle peaks are slightly broadened. In addition to the nuclear peaks, there are a number of magnetic peaks, which, as indicated in Fig. 2, can be assigned to a unit cell doubled in all directions with respect to the original cell. This is indicative of

TABLE III. Parameter values and standard errors from least-squares refinement of single-crystal data from RbFeF<sub>3</sub>.

	120 °K	95 °K	80 °K	55 °K	42 °K
<i>B</i> <sub>Rb</sub> (Å <sup>2</sup> )	0.53 ± 0.10	0.47 ± 0.12	0.43 ± 0.11	0.31 ± 0.09	0.19 ± 0.08
<i>B</i> <sub>Fe</sub> (Å <sup>2</sup> )	0.43 ± 0.10	0.36 ± 0.12	0.36 ± 0.11	0.29 ± 0.09	0.25 ± 0.08
<i>B</i> <sub>F</sub> (Å <sup>2</sup> )	0.73 ± 0.12	0.58 ± 0.13	0.57 ± 0.11	0.51 ± 0.10	0.28 ± 0.08
Extinction factor <i>g</i> (× 10 <sup>-4</sup> )	0.055 ± 0.014	0.036 ± 0.013	0.040 ± 0.011	0.026 ± 0.009	0.025 ± 0.008
<i>R</i> factor (%)	1.6	1.9	1.6	1.5	1.4
Weighted <i>R</i> factor (%)	1.4	1.6	1.4	1.2	1.2

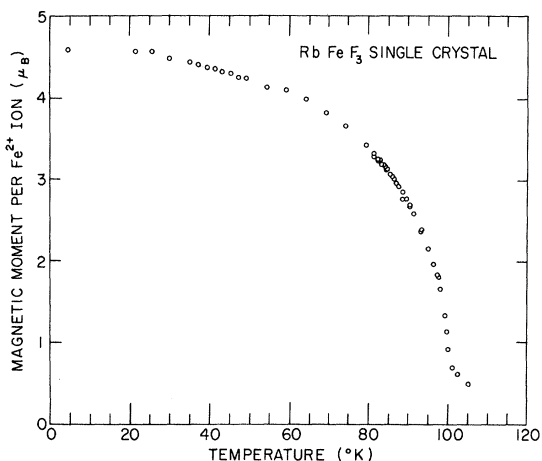


FIG. 4. Magnetic moment of  $\text{Fe}^{2+}$  as a function of temperature.

type-G collinear antiferromagnetic ordering, in which nearest-neighbor moments are coupled antiparallel. The magnetic moment determined from the intensity of the  $(\frac{1}{2}, \frac{1}{2}, \frac{1}{2})$  reflection with the calculated spin-only form factor<sup>15</sup> was found to have an extrapolated value of  $4.4 \pm 0.2 \mu_B$  at  $0^\circ\text{K}$ .

#### B. Single-Crystal Data

Single-crystal nuclear and magnetic intensity data were obtained at a number of temperatures. The only magnetic peaks observed were those expected from the G-type order. There was also a fairly sharp increase of several percent in the intensities of the "strong" nuclear peaks such as (200) as the temperature was lowered through the Néel point, followed by a more gradual increase down to  $40^\circ\text{K}$ . However, there was no corresponding increase in the intensities of weaker peaks such as (100), so that the possibility of any substantial ferromagnetic contribution must be ruled out. However, a least-squares analysis of the  $120^\circ\text{K}$  data indicated the presence of extinction effects, and an extinction parameter of the type proposed by Zachariasen<sup>16</sup> was introduced into the refinement. Individual isotropic temperature factors were also treated as variable parameters. Results are summarized in Table III, and the calculated and observed structure factors at  $120^\circ\text{K}$  and  $42^\circ\text{K}$  are compared in Table IV. There is a significant decrease in the magnitude of the extinction parameter as the temperature is lowered. It is reasonable to attribute this to the formation of domains and an increase in the mosaic spread caused by the lowering of the crystal symmetry at the various transitions. Some of the peaks were observed to be broadened at the lower temperatures.

$\text{Fe}^{2+}$  form factor values were determined from both single-crystal and powder data, and are shown

in Fig. 3. Agreement is excellent, and the points fall very close to the theoretical spin-only curve. The intensity of the  $(\frac{1}{2}, \frac{1}{2}, \frac{1}{2})$  magnetic peak was also followed as a function of temperature down to  $4.6^\circ\text{K}$ . The magnetic moment in  $\mu_B$  per Fe ion, calculated as before, is plotted against temperature in Fig. 4. Extinction corrections have been made, and in no case exceed 6% for this reflection. Standard deviations of the counting statistics are smaller than the points in the figure. The absolute value of the moment extrapolated to  $0^\circ\text{K}$  is  $4.6 \pm 0.2 \mu_B$ , in good agreement with the powder result. From the temperature dependence of the intensity data for the (100) reflection, it can be concluded that the ferromagnetic component is less than  $0.6 \mu_B$ , which is not inconsistent with magnetic measurements.

In the neighborhood of the Néel point, the sublattice magnetization, which is proportional to  $(I_{\frac{1}{2}\frac{1}{2}\frac{1}{2}})^{1/2}$ , was found to follow a critical-scattering relationship of the type

$$(I_{\frac{1}{2}\frac{1}{2}\frac{1}{2}})^{1/2} = C [1 - (T/T_N)]^\beta$$

over a comparatively wide temperature range (see Fig. 5) from  $100.1$  to  $84.0^\circ\text{K}$  [ $0.0045 \leq (1 - T/T_N) \leq 0.160$ ]. A least-squares analysis of the data in this region yielded values of  $100.53 \pm 0.02$  for  $T_N$  and  $0.329 \pm 0.004$  for  $\beta$ . Within error limits, this latter value has also been found in Mössbauer studies of  $\text{RbFeF}_3$ <sup>3</sup> and in a number of other antiferromagnetic materials, such as  $\text{RbMnF}_3$ <sup>17</sup> and  $\text{MnF}_2$ .<sup>18</sup> The error in  $T_N$  is a relative one, and the absolute error is in the region of  $0.5^\circ\text{K}$ .

A careful examination of the temperature dependence of  $M(T)$  in Fig. 4 does not reveal any abrupt anomaly indicative of the transitions at  $85$  and  $45^\circ\text{K}$ , although there is perhaps a small discontinuity in the former case. There is also no detectable difference in the heating or cooling cycles. Thus the behavior of the antiferromagnetic component does

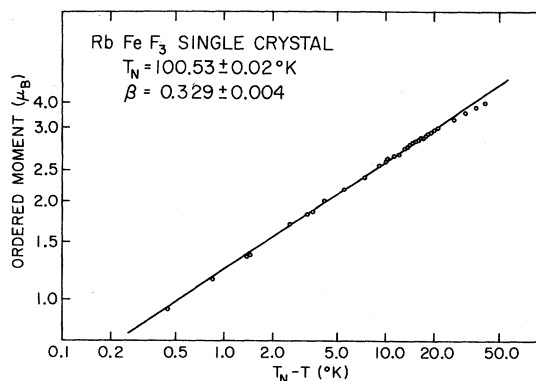


FIG. 5.  $(I_{\frac{1}{2}\frac{1}{2}\frac{1}{2}})^{1/2}$  as a function of  $(T_N - T)$  in the neighborhood of  $T_N$ .

not appear to be at all sensitive to the first-order transition.

Further elucidation of the magnetic structure below 86 °K will have to await a neutron diffraction study in an applied field, preferably with a polarized beam, which is currently being planned.

*Note added in proof.* A paper by J. B. Goodenough *et al.* [Phys. Rev. B **2**, 4640 (1970)] has recently come to our attention. This deals with the effects of hydrostatic pressure and Jahn-Teller distor-

tions on the magnetic properties of  $\text{RbFeF}_3$ , and presents a plausible explanation for many of the puzzling experimental observations previously reported.

#### ACKNOWLEDGMENTS

We wish to thank J. J. Hurst, Jr., Kedar Gupta, and Jahar Mukherjee for their valuable technical assistance.

<sup>†</sup>Work performed in part under the auspices of the U. S. Atomic Energy Commission.

\*Guest scientist at Brookhaven National Laboratory, Upton, N.Y. 11973.

<sup>1</sup>L. R. Testardi, H. J. Levinstein, and H. J. Guggenheim, Phys. Rev. Letters **19**, 503 (1967).

<sup>2</sup>Franklin F. Y. Wang and M. Kestigian, J. Appl. Phys. **37**, 975 (1966).

<sup>3</sup>G. K. Wertheim, H. J. Guggenheim, H. J. Williams, and D. N. E. Buchanan, Phys. Rev. **158**, 446 (1967).

<sup>4</sup>F. S. Chen, H. J. Guggenheim, H. J. Levinstein, and S. Singh, Phys. Rev. Letters **19**, 948 (1967).

<sup>5</sup>I. G. Sini, R. V. Pisarev, P. P. Symikov, G. A. Smolenskii, and A. I. Kapustin, Fiz. Tverd. Tela **10**, 2252 (1968) [Sov. Phys. Solid State **10**, 1775 (1969)].

<sup>6</sup>G. R. Hoy and S. Chandra, J. Chem. Phys. **47**, 961 (1967).

<sup>7</sup>G. K. Wertheim, H. J. Guggenheim, H. J. Williams, and D. N. E. Buchanan, J. Appl. Phys. **39**, 1253 (1968).

<sup>8</sup>U. Ganiel, M. Kestigian, and S. Shtrikman, Phys. Letters **A24**, 577 (1967).

<sup>9</sup>E. M. Gyorgy, H. J. Levinstein, J. F. Dillon, Jr., and H. J. Guggenheim, J. Appl. Phys. **40**, 1599 (1969).

<sup>10</sup>J. J. Hurst, K. P. Gupta, J. L. Mukherjee, D. E. Cox, and Franklin F. Y. Wang (unpublished).

<sup>11</sup>W. C. Hamilton, I. U. C. World List of Crystallographic Computer Programs, Program No. 313 (POWLS) (1962) (unpublished).

<sup>12</sup>Franklin F. Y. Wang and D. E. Cox, Acta Cryst. **A26**, 377 (1970); J. R. Copley, *ibid.* **A26**, 376 (1970); P. Meriel, Compt. Rend. **560B**, 270 (1970).

<sup>13</sup>C. G. Shull and Y. Yamada, J. Phys. Soc. Japan **17**, 1 (1962).

<sup>14</sup>M. J. Cooper and K. D. Rouse, Acta Cryst. **A26**, 214 (1970).

<sup>15</sup>R. E. Watson and A. J. Freeman, Acta Cryst. **14**, 27 (1961).

<sup>16</sup>W. H. Zachariasen, Acta Cryst. **23**, 558 (1967); P. Coppens and W. C. Hamilton, *ibid.* **A26**, 71 (1970).

<sup>17</sup>H. Y. Lau, L. M. Corliss, A. Delapalme, J. M. Hastings, R. Nathans, and A. Tucciarone, J. Appl. Phys. **41**, 1384 (1970).

<sup>18</sup>P. Heller and G. Benedek, Phys. Rev. Letters **8**, 428 (1962); P. Heller, Phys. Rev. **146**, 403 (1966).

## Green's-Function Analysis of the Ising Ferromagnet

F. Burr Anderson

Department of Physics, West Virginia University, Morgantown, West Virginia 26506

(Received 11 June 1970)

The method of the two-time temperature-dependent Green's function has been used to analyze the Ising model of a ferromagnet in an external magnetic field. The selection of a particular Green's function enables us to write an exact expression for the equation of motion. We are then led to a differential difference equation for the correlation function corresponding to the Green's function. No decoupling assumptions have been made, so the equation is exact for both arbitrary spin and range of interaction. It is shown how various approximate theories may be extracted from our formalism. The exact differential difference equation may be reduced to a partial differential equation. The latter form allows us to generate relations among the magnetization and spin-spin correlation functions. These relations are given in detail for the case of spin  $\frac{1}{2}$  and  $z$  nearest neighbors.

### I. INTRODUCTION

The method of the two-time temperature-dependent Green's function<sup>1</sup> has been used extensively to study magnetic systems based on the Heisen-

berg<sup>2-6</sup> and Ising<sup>7-11</sup> models. To obtain tractable solutions, decoupling procedures have been invoked to terminate the hierarchy of Green's functions generated by the equations of motion. In this paper we consider the Ising model of a ferromagnet with